Journal of Molecular Modeling (2019) 25: 154
https://doi.org/10.1007/s00894-019-4035-2

ORIGINAL PAPER

Quantum-chemical studies of homoleptic iridium(III) complexes in OLEDs: *fac* versus *mer* isomers

Izabela Grzelak[1] · Bartosz Orwat[1,2] · Ireneusz Kownacki[1,2] · Marcin Hoffmann[1]

Received: 30 November 2018 / Accepted: 15 April 2019 / Published online: 10 May 2019

Abstract

A series of facial ***fac*-[Ir(5-R-bzq)$_3$]** and meridional ***mer*-[Ir(5-R-bzq)$_3$]** Ir(III) complexes bearing benzo[*h*]quinoline-based ligands have been studied with the help of density functional theory (DFT) methods. A detailed electronic structure comparison of the two isomers has been addressed to point out the differences in their stability and photophysical properties. An influence of substituent impact on optical and electronic properties of Ir(III) homoleptic complexes was also explored by introducing into the cyclometalated ligands substituents characterized with different electronic properties, e.g., R = H, F, OPh, NMe_2, C_6F_5, and *p*-C_6H_4-NPh_2. The results herein show that *fac* and *mer* isomers exhibit remarkable differences in stability and photophysical properties. The introduction of different functional groups into bzq ligands, despite very similar geometrical structures, significantly affected HOMO and LUMO energy levels and energy gaps of the examined Ir(III) complexes.

Keywords Ir(III) complexes · DFT · Fac–mer isomer factors · Substitution effects · Organic light-emitting diodes

Introduction

Phosphorescent transition-metal complexes have recently caught significant attention because of their unique photophysical properties, which are useful in applications, such as dopants for OLEDs (organic light-emitting diode) [1–5], light-emitting electrochemical cells (LECs) [6–9], dye-sensitized solar cells [3, 10], water splitting [11, 12], and biological phosphorescent labels and sensors [13, 14]. Those complexes exhibit phosphorescence due to very strong spin–orbit coupling, which causes mutual isoenergetic transition from the singlet to the triplet state and conversely, known as intersystem crossing (ISC) [15]. Many families of heavy metal complexes, such as Os(II) [16], Ru(II) [17], Pt (II) [17], and Ir(III) [18–20], have been extensively investigated with the aim of better understanding their photophysical properties. In particular, cyclometalated iridium(III) complexes are very promising for a large range of luminescence-based applications because of their high photoluminescence quantum yields, relatively short excited-state lifetime, and general thermal and electrochemical stability [21–59]. Another interesting feature is the possibility of tuning the emission energy of Ir(III) complexes from blue to red light over the entire visible range, which is a key step for realizing the full-color displays and large-area solid-state lighting in OLED fields [4, 5, 19]. Emission color tuning is possible by varying emitter's HOMO–LUMO gap [60], either by using various ligand cores or playing with acceptor/donor character of the substituents on the main or the ancillary ligands.

In recent years, a number of intensive studies have been carried out to design and synthesize phosphorescent materials for highly efficient OLEDs. Nevertheless, most of the studies concerning this subject have been focused on the synthesis and photophysical properties of neutral and ionic iridium(III) compounds, those stabilized with various types of cyclometalated ligands built on the basis of 2-phenylpyridine (ppy) cores [61]. However, there has been little attention paid to iridium(III) compounds containing

This paper belongs to Topical Collection 8th conference on Modeling & Design of Molecular Materials (MDMM 2018)

Electronic supplementary material The online version of this article (https://doi.org/10.1007/s00894-019-4035-2) contains supplementary material, which is available to authorized users.

✉ Izabela Grzelak
izabela.grzelak@amu.edu.pl

[1] Faculty of Chemistry, Adam Mickiewicz University in Poznan, St. Umultowska 89b, 61-614 Poznan, Poland

[2] Center for Advanced Technologies, Adam Mickiewicz University in Poznan, St. Umultowska 89c, 61-614 Poznan, Poland

cyclometalating ligands, such as benzo[*h*]quinoline (bzq), which is an analogue of ppy [62]. This fact has prompted us to focus on homoleptic iridium(III) compounds with bzq ligands. They are termed homoleptic when three identical chelating ligands are present in the complex structure as illustrated below.

Furthermore, there are two possible isomers, facial and meridional (*fac* and *mer*), for such complexes having three identical but unsymmetrical bidentate ligands [63–66] (Fig. 1).

In this work, we present a series of iridium(III) complexes with three cyclometalating ligands based on bzq. We report herein an extensive theoretical investigation of the structural, electrochemical, and photophysical properties of these compounds. A systematic comparison of *fac* and *mer* isomer pairs aimed at identification of the differences in their stability and photophysical properties is presented. In addition, as HOMO and LUMO energy levels are likely to be affected by the substitution effects, we were interested in red or blue shifts in the emissions of these *fac* and *mer* Ir(III) complexes.

Computational details and theory

The ground-state geometries were fully optimized using the density functional theory (DFT) [67] with B3LYP [68–70], M06 [71], and WB97XD [72] functionals. These methods were selected on the basis of the results from extensive comparative studies, they are also recommended for robust and fast calculations for large organometallic compounds [68–72]. The 6-31G(d,p) basis set was used for H, C, N, O, and F atoms [73] and LANL2DZ basis set was adopted for the Ir atom [74]. A relativistic effective core potential (ECP) on Ir replaced the inner core electrons leaving the outer core ($5s^25p^6$) electrons and the valence electrons ($5d^6$) of Ir(III). There were no symmetry constraints on these Ir(III) complexes during the geometry optimizations. Vibrational analyses for the optimized structures of isolated molecules were performed to verify if a given structure corresponded to potential energy minima and to calculate zero-point vibrational energies, entropies, and thermal corrections for Gibbs free energies. Solvent–solute interactions were taken into account with the aid of the polarizable continuum model (PCM) [75–77] and acetonitrile or dichloromethane as the solvent usually used in experimental studies [78, 79]. All calculations were carried out with Gaussian09 software package [80] in PL-Grid infrastructure.

In this paper, we focused our attention on several R-substituted (R = H, F, OMe, OPh, NMe_2, C_6F_5, and p-C_6H_4-NPh_2) Ir(5-R-bzq)$_3$ complexes in both *fac* and *mer* isomeric forms. These tris–cyclometalated Ir(III) complexes were studied to explore preferences toward *fac* or *mer* isomers of Ir(III) complexes.

Results and discussion

Geometries in the ground state (S_0)

The representative optimized structures of *fac*-[Ir(bzq)$_3$] and *mer*-[Ir(bzq)$_3$] in the ground state (S_0) along with the numbering of some key atoms are shown in Fig. 2. In order to investigate the solvent effect, the ground-state geometry optimization was also carried out within the PCM method [75–77]. The selected optimized geometry parameters for [Ir(bzq)$_3$] in the gas phase and the acetonitrile environment are summarized in Table 1S (Supplementary materials).

Table 1S (Supplementary materials) illustrates the parameters of Ir–ligand bond lengths and bond angles in the gas phase and CH_3CN media for [Ir(bzq)$_3$]. Calculated Ir–N, Ir–C, and

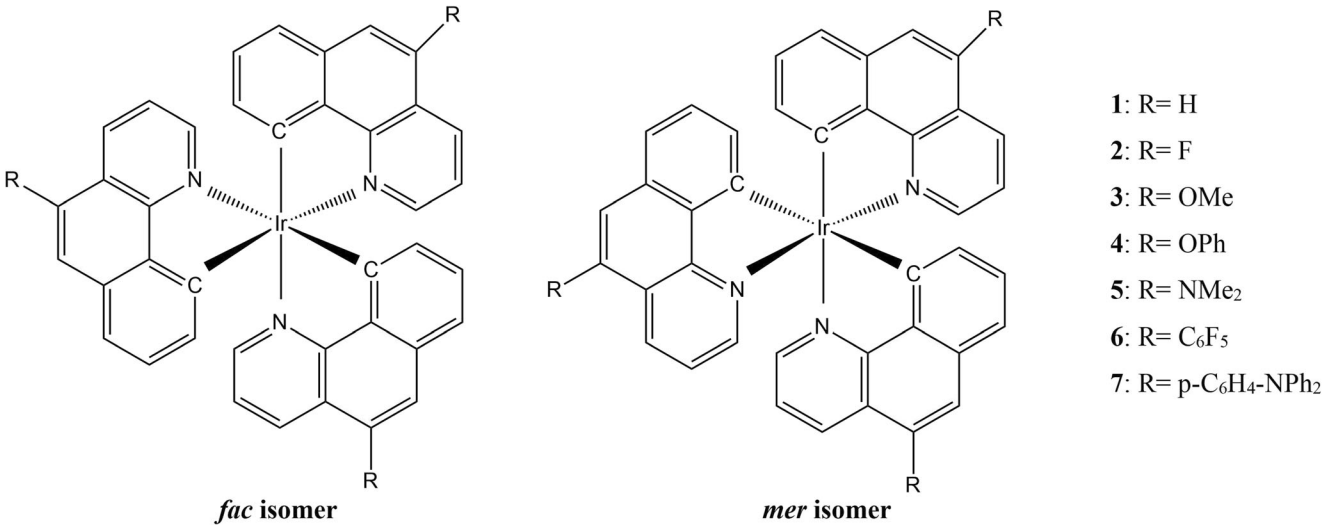

Fig. 1 Chemical formulas of Ir(III) complexes examined

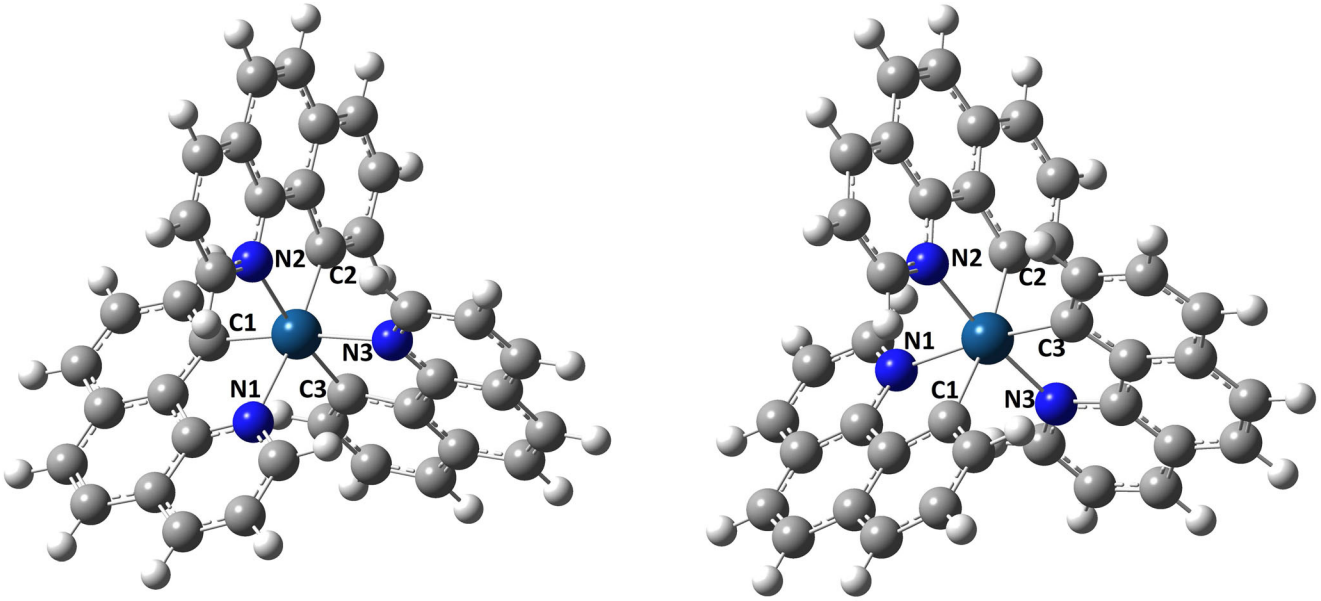

Fig. 2 Optimized geometries of *fac*-[Ir(bzq)$_3$] and *mer*-[Ir(bzq)$_3$] in the ground state

Ir–O bond lengths are slightly larger in the gas phase than in the acetonitrile environment. The maximum deviation in bond distances between coordinating atoms and Ir(III) is 0.008 Å, while changes in bond angles are less than 1.0°. However, the geometries of all complexes present similar features, indicating that the solvent environment has little effect on the geometry of the complexes.

The optimized structures showed the expected pseudo-octahedral coordination geometry around the iridium center (the corresponding parameters provided as Supplementary material). According to Fig. 2 and Table 1S, two coordinated atoms (N(2) and C(3)) in the *fac* isomer are in *trans* position and the valence angle of N(2)–Ir–C(3) is nearly 180°, while the coordinating atoms (N(3) and C(2)) are in *cis* position and the valence angle value N(3)–Ir–C(2) is close to 90°. Furthermore, two valence angles between the coordinating atoms from the same ligand and the central iridium atom N(2)–Ir–C(1) and N(1)–Ir–C(3) are nearly identical, ca. 90° (Table 1S and Fig. 1). Likewise, the valence angles N(2)–Ir–N(1) and C(1)–Ir–C(3) in the *mer* isomer are also ca. 90°. For *fac*-[Ir(bzq)$_3$], Ir–N bonds lengths (Ir–N1, Ir–N2, Ir–N3) are in the range of 2.195 – 2.199 Å, while Ir–C bonds (Ir–C1, Ir–C2, Ir–C3) vary from 2.033 to 2.035 Å (Table 1). It was found that Ir–C bond lengths are significantly shorter by ~0.15 Å compared to Ir–N bonds. A similar electronic environment of Ir–C/Ir–N bonds leads to their similar bond distance (0.002 Å and 0.004 Å). It is also notable that the change of substituent (R = H, F, OMe, OPh, NMe_2, C_6F_5, and p-C_6H_4-NPh_2) in position 5 in bzq ligand very slightly affects Ir–C and Ir–N bond lengths of *fac* complexes containing these functionalized ligands.

In the case of complex *mer*-[Ir(bzq)$_3$], Ir–C and Ir–N bond lengths are different from those in the *fac* isomer. In *mer* configuration, two donor carbon atoms (C1 vs. C2) and two donor nitrogen atoms (N2 vs. N3) adopt a *trans* orientation, leaving the remaining C3 and N1 atoms *trans* to each other. The different local environments result in different bond lengths for these Ir–C and Ir–N bonds. For instance, owing

Table 1 Selected calculated bond distances (Å) in the ground states (S_0) for the studied complexes

	1		2		3		4		5		6		7	
	fac	*mer*	*fac*	*mer*	*fac*	*mer*	*fac*	*mer*	*fac*	*mer*	*fac*	*mer*	*fac*	*mer*
Ir–C1	2.035	2.117	2.035	2.117	2.033	2. 117	2.034	2.116	2.034	2.115	2.034	2.114	2.033	2.113
Ir–C2	2.035	2.106	2.035	2.106	2.034	2.105	2.034	2.104	2.033	2.102	2.033	2.101	2.033	2.102
Ir–C3	2.035	2.024	2.035	2.025	2.034	2.024	2.035	2.024	2.035	2.023	2.033	2.022	2.033	2.022
Ir–N1	2.197	2.215	2.196	2.215	2.196	2.215	2.196	2.215	2.197	2.216	2.196	2.215	2.196	2.214
Ir–N2	2.197	2.078	2.198	2.078	2.198	2.078	2.198	2.078	2.197	2.078	2.195	2.078	2.195	2.078
Ir–N3	2.197	2.089	2.198	2.089	2.199	2.090	2.199	2.091	2.197	2.092	2.198	2.092	2.196	2.083

to the strong *trans* influence of carbon atom C3, Ir–N bond (Ir–N1) *trans* to it is much longer (about 0.13 Å) than the other two Ir–N ones (Ir–N2, Ir–N3, see Table 1 and Fig. 2). It was also found that Ir–C and Ir–N bond distances follow the trend: Ir–C1 > Ir–C2 > Ir–C3 and Ir–N1 > Ir–N3 > Ir–N2. Moreover, hardly any variation in Ir–C and Ir–N bond lengths (the differences are 0.005 Å and 0.004 Å) was observed upon the substituent change in position 5 of these *mer* complexes.

On the basis of the obtained Gibbs free energies for iridium(III) complexes, populations of conformers were calculated using a standard Boltzmann formalism. The percentage of a conformer X is given as:

$$\%X = \frac{\exp\left(-\frac{\Delta G_x^0}{RT}\right)}{\sum_i \exp\left(-\frac{\Delta G_i^0}{RT}\right)} \times 100\% \quad (1)$$

where $\Delta G_x{}^0$ is the relative energy of a conformer X.

The relative free energies of the optimized conformations in the ground state along with their distributions are summarized in Table 2. In all cases, the most energetically preferred structure was the *fac* configuration. The relative energy of *fac*-[Ir(5-R-bzq)$_3$] in comparison to the *mer*-[Ir(5-R-bzq)$_3$] was more favorable from about 8 kcal mol^{-1} to 9.2 kcal mol^{-1}. As we can see, the *fac* isomer is more stable than *mer*, which is consistent with the experimental observations for similar ppy-based complexes [81]. The calculated populations of conformers suggest that virtually only the facial isomers are likely to be observed in the equilibrium.

NMR chemical shifts

The ^{1}H NMR calculations were carried out for the two isomers of complex [Ir(bzq)$_3$] in CH_2Cl_2 solvent using PCM model and compared to experimental ^{1}H chemical shifts reported in literature [81]. It must be underlined here that experimental data relate to a mixture of isomers [82] because the isolation of pure facial or meridional isomer was not achieved; as reported by Lamansky et al. [81]: "The Ir(bzq)$_3$ product from this reaction is a mixture of *fac*- and *mer*-isomers. Several wash cycles (acetone and dichloromethane) cause significant enrichment of the mixture in fac-product but still does not allow isolation of a pure facial complex.". Therefore, the experimental data was compared with computational data obtained for both isomers (Table 3). The spectral data of the complexes *fac*-[Ir(bzq)$_3$] and *mer*-[Ir(bzq)$_3$] have been summarized in Table 2S and Table 3S (Supplementary materials).

Table 2 Comparison of *fac*/*mer* relative energies in the ground state obtained in B3LYP calculations and population of obtained conformers

Species	Conformer	Relative energy in vacuum [kcal mol^{-1}]] B3LYP/GEN	Entropy [cal mol^{-1} ∗K] B3LYP/GEN	Thermal correction to G [hartree] B3LYP/GEN	Solvation correction to G [hartree] B3LYP/GEN	Relative ΔG [kcal mol^{-1}] B3LYP/GEN	Population of conformers X [%]
1	*fac*	0[a]	193.690	0.458803	−0.015587	0	>99.9
	mer	8.8	192.757	0.459205	−0.014579	9.1	<0.1
2	*fac*	0[b]	206.874	0.430771	−0.014756	0	>99.9
	mer	8.9	205.930	0.431161	−0.013616	9.2	<0.1
3	*fac*	0[c]	231.231	0.546774	−0.017932	0	>99.9
	mer	9.2	230.219	0.547219	−0.018567	9.4	<0.1
4	*fac*	0[d]	294.705	0.681898	−0.016932	0	>99.9
	mer	7.9	293.201	0.680728	−0.017243	8.4	<0.1
5	*fac*	0[e]	251.058	0.662387	−0.018438	0	>99.9
	mer	8.9	249.993	0.662842	−0.017271	9.2	<0,1
6	*fac*	0[f]	248.126	0.66722	−0.195789	0	>99.9
	mer	7.9	336.044	0.638312	−0.186478	8.6	<0.1
7	*fac*	0[g]	436.178	1.161229	−0.029694	0	>99.9
	mer	8.0	435.391	1.160379	−0.028532	9.1	<0.1

Absolute energy baselines [in hartree]:

[a] 1769.811996

[b] 2067.526347

[c] 2111.509138

[d] 2689.066343

[e] 2171.723886

[f] 3948.794651

[g] 4011.872968

Table 3 Calculated 1H NMR chemical shifts (ppm) together with the experimental data for *fac*-[Ir(bzq)$_3$] and *mer*-[Ir(bzq)$_3$]

Experimental[a]	Calculated
8.31	8.31 (H14, *mer*)
8.19	8.22 (H7, *mer*)
8.12	8.12 (H2, *mer*)
8.03	8.03 (H4, *fac*)
7.90	7.85 (H17, *mer*)
7.60	7.67 (H10, *mer*)
7.47	7.67 (H13, *mer*)
7.39	7.53 (H2, *fac*)
7.22	7.50 (H20, *mer*)
7.14	7.49 (H6, *mer*)
7.07	7.46 (H24, *mer*)
6.96	7.46 (H15, *mer*)
6.8	7.39 (H8, *fac*)
6.57	7.18 (H8, *mer*)

[a] Ref. [81]

As shown in Fig. 1S (Supplementary materials), calculated chemical shifts of ^{1}H NMR spectra for *fac*-[Ir(bzq)$_3$] and *mer*-[Ir(bzq)$_3$] are in good agreement with the experimental data, the obtained correlation equaled 0.95. The comparison of calculated and experimental data let us assume that signals in experimental spectrum come from both isomers. In the ^{1}H NMR spectrum of *fac*-[Ir(bzq)$_3$], eight protons of a single bzq ligand are displayed because the three ligands surrounding the iridium atom are magnetically equivalent. The signals appearing at 8.03 ppm, 7.53 ppm, and 7.39 ppm originate from *fac*-[Ir(bzq)$_3$] and the other signals originate from *mer*-[Ir(bzq)$_3$].

Frontier molecular orbitals analysis

Results from numerous literature reports indicated that frontier molecular orbitals analysis constitutes a useful proxy for experimentally recorded photophysical properties of iridium(III) complexes [78, 79, 82–84]. It is known that frontier molecular orbitals (FMO) of complex ground state S_0 are related to its spectral properties [86]. Emission color of iridium(III) complexes can be adjusted by changing their HOMO–LUMO bandgap, which can be achieved on the course of ligand functionalization with electron-donating and electron-withdrawing substituents [86], and values of HOMO–LUMO gaps predicted for Ir(III) complexes by DFT methods showed surprisingly good correlation with the experimentally recorded values of energies of emitted photons even in the case of phosphorescence, see for example [21, 22, 83–85, 87–90]. Contour plots of frontier orbitals of both [Ir(bzq)$_3$] isomers are depicted in Fig. 3, while the visualizations of complexes 2–7 are collected in Table 4S (Supplementary materials).

As shown in Fig. 3, HOMO of *fac*-[Ir(bzq)$_3$] is predominantly localized on the iridium atom and over benzo moieties of the three bzq ligands. Similarly, LUMO is localized mostly on pyrido fragments of the bzq ligands. It is also noteworthy that change of the substituent in position 5 (R = H, F, OMe, OPh, NMe_2, C_6F_5, and p-C_6H_4–NPh_2) causes minor effects

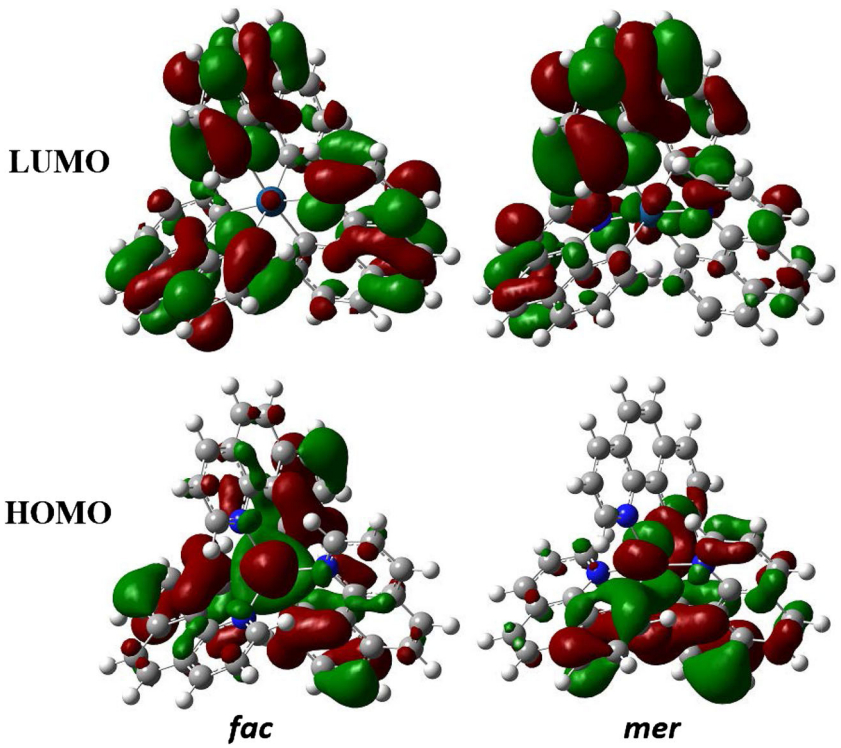

Fig. 3 Contour plots of HOMOs (bottom) and LUMOs (top) of *fac*-[Ir(bzq)$_3$] (left) and *mer*-[Ir(bzq)$_3$] (right)

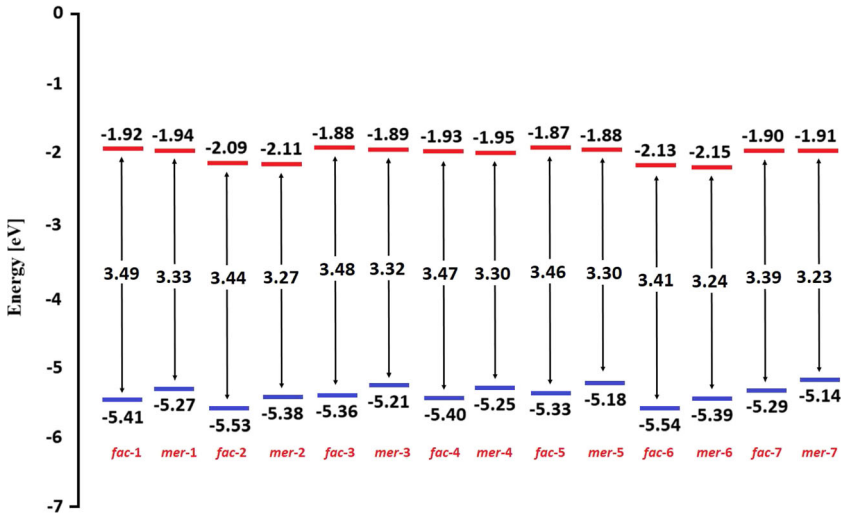

Fig. 4 Energy levels and HOMO–LUMO energy gaps of the studied complexes (in eV) calculated at the B3LYP/LANL2DZ/6-311++G(d,p) level of theory

on the electron densities of the HOMOs and LUMOs of complexes 1–7 (Supplementary material).

In the case of *mer* isomers, HOMO dominants residues on Ir metal center and benzo moieties of two bzq ligands containing C1 and C3 donor atoms. LUMO of *mer*-[Ir(bzq)$_3$] is mainly spread over pyrido moieties of the bzq ligands containing N1 and N2 donor atoms. Similarly, as in the case of *fac*-[Ir(bzq)$_3$], HOMO and LUMO distributions seem not to be very sensitive to substituents influence.

Energy levels of frontier orbitals and HOMO–LUMO energy gap for studied complexes are plotted in Fig. 4. It can be seen that the impact of R substituent variation on HOMO and LUMO energy levels for *fac*-[Ir(5-R-bzq)$_3$] series follows the same trend as in the case of *mer*-[Ir(5-R-bzq)$_3$] series. In general, electron-withdrawing substituents (R = F, C_6F_5) are responsible for lowering energy levels of HOMO and LUMO, but does not extend the HOMO–LUMO energy gap in comparison to unmodified [Ir(bzq)$_3$]. According to that, electron-donating groups (R = OMe, OPh, NMe_2, and p-C_6H_4–NPh_2) cause a higher increase of HOMO and LUMO levels in reference to unmodified [Ir(bzq)$_3$]. In addition, such substituents induce more destabilization of HOMO than LUMO, resulting in smaller HOMO–LUMO energy gaps (E_g).

Moreover, it should also be pointed out that LUMO levels of complexes in *fac* configuration are similar to their *mer* analogues, while HOMO energy is decreased in comparison to *mer* isomers, thereby leading to larger energy gaps of *fac*-[Ir(5-R-bzq)$_3$] than the corresponding *mer*-[Ir(5-R-bzq)$_3$] (Fig. 4). The energies of FMOs calculated with the use of different methods were listed in Tables 5S–7S in Supplementary materials.

Conclusions

Electronic structures and photophysical properties of facial and meridional Ir(III) complexes (*fac*-[Ir(5-R-bzq)$_3$] and *mer*-[Ir(5-R-bzq)$_3$]) series were examined with the use of density functional theory. For all of the studied iridium complexes, a greater thermodynamic stability of *fac* isomers in reference to *mer* isomers were observed. DFT calculation with different functionals (B3LYP, M06, and WB97XD) showed approximately 9 kcal mol^{-1} stabilization of total energy in favor of *fac* isomers. The differences in the ligand orientation around the metal center causes the HOMO energies of meridional isomers to be higher than those of facial forms, while LUMO energies are roughly the same. Consequently, HOMO–LUMO energy gaps are wider for *fac*-[Ir(5-R-bzq)$_3$] than the corresponding *mer*-[Ir(5-R-bzq)$_3$]. The obtained results show that geometrical structures of the complexes are hardly affected by change of substituent (R = H, F, OPh, NMe_2, C_6F_5, and p-C_6H_4–NPh_2) in position 5 of cyclometalated ligand, while HOMO and LUMO energy levels are significantly influenced by the substitution effects. In particular, the incorporation of electron-donating substituent p-C_6H_4–NPh_2 leads to decreased HOMO–LUMO gap, thus suggesting red shift on the absorption/emissions spectra lines. In addition, the predicted change of HOMO and LUMO energy levels for both *fac* and *mer* forms are similar. Moreover, we suggested which signals in ^{1}H NMR spectra are likely to correspond to *fac* or *mer* isomers, which should help in interpretation of experimental NMR spectra.

Acknowledgments This work was supported by the National Science Centre (Poland) through grant no. UMO-2013/11/B/ST5/01334. This research was supported in part by PL-Grid Infrastructure.

Author contributions The manuscript was written through contributions of all authors. All authors have given approval to the final version of the manuscript.

Compliance with ethical standards

Competing interests The authors declare no competing financial interest.

Abbreviations OLED, Organic light-emitting diode; ISC, Intersystem crossing; PLQY, Photoluminescence quantum yield; FMO, Frontier molecular orbitals; HOMO, Highest occupied molecular orbital; LUMO, Lowest occupied molecular orbital; DFT, Density functional theory; NMR, Nuclear magnetic resonance

References

1. Flamigni L, Barbieri A, Sabatini C et al (2007) Photochemistry and photophysics of coordination compounds: iridium. Photochemistry and Photophysics of coordination compounds II. Springer, Berlin, pp 143–203
2. You Y, Park SY (2009) Phosphorescent iridium(III) complexes: toward high phosphorescence quantum efficiency through ligand control. Dalton Trans 8:1267–1282. https://doi.org/10.1039/B812281D
3. Baranoff E, Yum J-H, Graetzel M, Nazeeruddin MK (2009) Cyclometallated iridium complexes for conversion of light into electricity and electricity into light. J Organomet Chem 694: 2661–2670. https://doi.org/10.1016/j.jorganchem.2009.02.033
4. Chi Y, Chou P-T (2010) Transition-metal phosphors with cyclometalating ligands: fundamentals and applications. Chem Soc Rev 39:638–655. https://doi.org/10.1039/b916237b
5. Ulbricht C, Beyer B, Friebe C et al (2009) Recent developments in the application of phosphorescent iridium(III) complex systems. Adv Mater 21:4418–4441. https://doi.org/10.1002/adma.200803537
6. Costa RD, Ortí E, Bolink HJ et al (2012) Luminescent ionic transition-metal complexes for light-emitting electrochemical cells. Angew Chem Int Ed Eng 51:8178–8211. https://doi.org/10.1002/anie.201201471
7. Hu T, He L, Duan L, Qiu Y (2012) Solid-state light-emitting electrochemical cells based on ionic iridium(III) complexes. J Mater Chem 22:4206–4215. https://doi.org/10.1039/C2JM16185K
8. Hasan K, Donato L, Shen Y et al (2014) Cationic iridium(III) complexes bearing ancillary 2,5-dipyridyl(pyrazine) (2,5-dpp) and 2,2′:5′,2″-terpyridine (2,5-tpy) ligands: synthesis, optoelectronic characterization and light-emitting electrochemical cells. Dalton Trans 43: 13672–13682. https://doi.org/10.1039/C4DT02100B
9. Sun L, Galan A, Ladouceur S et al (2011) High stability light-emitting electrochemical cells from cationic iridium complexes with bulky 5,5′ substituents. J Mater Chem 21:18083–18088. https://doi.org/10.1039/C1JM12984H
10. Ning Z, Zhang Q, Wu W, Tian H (2009) Novel iridium complex with carboxyl pyridyl ligand for dye-sensitized solar cells: high fluorescence intensity, high electron injection efficiency? J Organomet Chem 694: 2705–2711. https://doi.org/10.1016/j.jorganchem.2009.02.016
11. Curtin PN, Tinker LL, Burgess CM et al (2009) Structure-activity correlations among iridium(III) photosensitizers in a robust water-reducing system. Inorg Chem 48:10498–10506. https://doi.org/10.1021/ic9007763
12. McDaniel ND, Coughlin FJ, Tinker LL, Bernhard S (2008) Cyclometalated iridium(III) Aquo complexes: efficient and tunable catalysts for the homogeneous oxidation of water. J Am Chem Soc 130:210–217. https://doi.org/10.1021/ja074478f
13. Lo KK-W, Li SP-Y, Zhang KY (2011) Development of luminescent iridium(III) polypyridine complexes as chemical and biological probes. New J Chem 35:265–287. https://doi.org/10.1039/C0NJ00478B
14. You Y, Nam W (2012) Photofunctional triplet excited states of cyclometalated Ir(III) complexes: beyond electroluminescence. Chem Soc Rev 41:7061–7084. https://doi.org/10.1039/c2cs35171d
15. Xu F, Kim J-H, Kim HU et al (2013) Phosphorescent organic light-emitting diodes fabricated using iridium complexes with carbazole-based benzothiazole ligands. Synth Met 178:10–17. https://doi.org/10.1016/j.synthmet.2013.06.023
16. Tung Y-L, Wu P-C, Liu C-S et al (2004) Highly efficient red phosphorescent osmium(II) complexes for OLED applications. Organometallics 23:3745–3748. https://doi.org/10.1021/om0498246
17. Xiang H-F, Chan S-C, KK-Y W et al (2005) High-efficiency red electrophosphorescence based on neutral bis(pyrrole)-diimine platinum(II) complex. Chem Commun 0:1408–1410. https://doi.org/10.1039/B415711G
18. Lamansky S, Djurovich P, Murphy D et al (2001) Highly phosphorescent Bis-Cyclometalated iridium complexes: synthesis, Photophysical characterization, and use in organic light emitting diodes. J Am Chem Soc 123:4304–4312. https://doi.org/10.1021/ja003693s
19. Xiao L, Chen Z, Qu B et al (2011) Recent progresses on materials for electrophosphorescent organic light-emitting devices. Adv Mater 23:926–952. https://doi.org/10.1002/adma.201003128
20. Chen Z, Bian Z, Huang C (2010) Functional IrIII complexes and their applications. Adv Mater 22:1534–1539. https://doi.org/10.1002/adma.200903233
21. Benjamin H, Fox MA, Batsanov AS et al (2017) Pyridylpyrazole N^N ligands combined with sulfonyl-functionalised cyclometalating ligands for blue-emitting iridium(III) complexes and solution-processable PhOLEDs. Dalton Trans 46:10996–11007. https://doi.org/10.1039/C7DT02289A
22. Kim HU, Sohn S, Choi W et al (2018) Substituents engineered deep-red to near-infrared phosphorescence from tris-heteroleptic iridium(III) complexes for solution processable red-NIR organic light-emitting diodes. J Mater Chem C 6:10640–10658. https://doi.org/10.1039/C8TC04321C
23. Escudero D (2016) Quantitative prediction of photoluminescence quantum yields of phosphors from first principles. Chem Sci 7: 1262–1267. https://doi.org/10.1039/C5SC03153B
24. Urinda S, Das G, Pramanik A, Sarkar P (2018) Essential role of ancillary ligand in color tuning and quantum efficiency of Ir(III) complexes with N-heterocyclic or Mesoionic Carbene ligand: a comparative quantum chemical study. J Phys Chem A 122:7532–7539. https://doi.org/10.1021/acs.jpca.8b05376
25. Urinda S, Das G, Pramanik A, Sarkar P (2017) Quantum chemical investigation on the Ir(III) complexes with an isomeric triazine-based imidazolium carbene ligand for efficient blue OLEDs. Phys Chem Chem Phys 19:29629–29640. https://doi.org/10.1039/C7CP03299D
26. Escudero D, Jacquemin D (2015) Computational insights into the photodeactivation dynamics of phosphors for OLEDs: a perspective. Dalton Trans 44:8346–8355. https://doi.org/10.1039/C4DT03804E
27. Urinda S, Das G, Pramanik A, Sarkar P (2016) Theoretical studies on the photophysical properties of some iridium (III) complexes used for OLED. J Phys Chem Solids 96–97:100–106. https://doi.org/10.1016/j.jpcs.2016.05.006
28. Avilov I, Minoofar P, Cornil J, De Cola L (2007) Influence of substituents on the energy and nature of the lowest excited states of heteroleptic phosphorescent Ir(III) complexes: a joint theoretical and experimental study. J Am Chem Soc 129:8247–8258. https://doi.org/10.1021/ja0711011
29. Urinda S, Das G, Pramanik A, Sarkar P (2016) Tuning the phosphorescence and quantum efficiency of heteroleptic Ir(III)

complexes based on pyridine-tetrazole as an ancillary ligand: an overview from quantum chemical investigations. Comput Theor Chem 1092:32–40. https://doi.org/10.1016/j.comptc.2016.07.025
30. De Angelis F, Fantacci S, Evans N et al (2007) Controlling phosphorescence color and quantum yields in cationic iridium complexes: a combined experimental and theoretical study. Inorg Chem 46:5989–6001. https://doi.org/10.1021/ic700435c
31. Guo J, Pan X, Wang X et al (2018) Theoretical study on the vibrationally resolved spectra and quantum yield of blue phosphorescent iridium(III) complexes with 2-(4-fluoro-3-(trifluoromethyl)-phenyl)pyridine as the cyclometalated ligand. Org Electron 61:125–133. https://doi.org/10.1016/j.orgel.2018.06.055
32. Liu Y, Hao Z, Meng F et al (2018) Efficient near-infrared emission of π-extended cyclometalated iridium complexes based on pyrene in solution-processed polymer light-emitting diode. Chem Phys Lett 699:99–106. https://doi.org/10.1016/j.cplett.2018.03.046
33. Liao J-L, Devereux LR, Fox MA et al (2018) Role of the diphosphine chelate in emissive, charge-neutral iridium(III) complexes. Chem Eur J 24:624–635. https://doi.org/10.1002/chem.201703482
34. Tong B, Wang H, Chen M et al (2018) High efficiency green OLEDs based on homoleptic iridium complexes with steric phenylpyridazine ligands. Dalton Trans 47:12243–12252. https://doi.org/10.1039/C8DT02781A
35. Choi HJ, Hyun MH, Park HJ, Yoon UC (2017) Synthesis of efficient blue phosphorescent heteroleptic Ir(III) complexes containing 4-alkoxy- or 4-alkylaminopicolinates as ancillary ligands. J Lumin 188:323–330. https://doi.org/10.1016/j.jlumin.2017.04.043
36. Benjamin H, Liang J, Liu Y et al (2017) Color tuning of efficient electroluminescence in the blue and green regions using Heteroleptic iridium complexes with 2-Phenoxyoxazole ancillary ligands. Organometallics 36:1810–1821. https://doi.org/10.1021/acs.organomet.7b00161
37. Sree VG, Cho W, Shin S et al (2017) Highly efficient solution-processed deep-red emitting heteroleptic thiophene-phenylquinoline based Ir(III) complexes for phosphorescent organic light-emitting diodes. Dyes Pigments 139:779–787. https://doi.org/10.1016/j.dyepig.2017.01.004
38. Wang X, Feng S, Wang X et al (2017) Theoretical insights into the phosphorescent process of a series of 2-(2-trifluoromethyl) pyrimidine-pyridine based heteroleptic iridium(III) compounds: the influence of the ancillary ligand. Comput Theor Chem 1105: 69–76. https://doi.org/10.1016/j.comptc.2017.02.026
39. Li J, Wang L, Wang X et al (2017) Theoretical perspective of FIrpic derivatives: relationship between structures and photophysical properties. Spectrochim Acta A Mol Biomol Spectrosc 171:425–431. https://doi.org/10.1016/j.saa.2016.08.021
40. Liu B, Dang F, Feng Z et al (2017) Novel iridium(III) complexes bearing dimesitylboron groups with nearly 100% phosphorescent quantum yields for highly efficient organic light-emitting diodes. J Mater Chem C 5:7871–7883. https://doi.org/10.1039/C7TC02369C
41. Duan Y-C, Wu Y, Ren X-Y et al (2017) From blue to full color – theoretical design and characterization of a series of Ir(III) complexes containing azoline ligand with potential application in OLEDs. Dalton Trans 46:11491–11502. https://doi.org/10.1039/C7DT02684F
42. Cho Y-J, Kim S-Y, Kim J-H et al (2017) Probing photophysical properties of isomeric N-heterocyclic carbene Ir(III) complexes and their applications to deep-blue phosphorescent organic light-emitting diodes. J Mater Chem C 5:1651–1659. https://doi.org/10.1039/C6TC04757B
43. Kuo H-H, Chen Y-T, Devereux LR et al (2017) Bis-tridentate Ir(III) metal phosphors for efficient deep-blue organic light-emitting diodes. Adv Mater 29:1702464. https://doi.org/10.1002/adma.201702464
44. Elie M, Renaud J-L, Gaillard S (2018) N-heterocyclic carbene transition metal complexes in light emitting devices. Polyhedron 140: 158–168. https://doi.org/10.1016/j.poly.2017.11.045
45. Zhang Q, Wang X, Zhang Y et al (2016) Insight into the phosphorescent process of Cyclometalated Ir(III) complexes: combination of the substituents on primary and ancillary ligands controls the emission rule and quantum yield. J Phys Chem C 120:27523–27532. https://doi.org/10.1021/acs.jpcc.6b07562
46. Li T-Y, Wu J, Wu Z-G et al (2018) Rational design of phosphorescent iridium(III) complexes for emission color tunability and their applications in OLEDs. Coord Chem Rev 374:55–92. https://doi.org/10.1016/j.ccr.2018.06.014
47. Liu X, Yao B, Wang H et al (2018) Efficient solution-processed yellow/orange phosphorescent OLEDs based on heteroleptic Ir(III) complexes with 2-(9,9-diethylfluorene-2-yl)pyridine main ligand and various ancillary ligands. Org Electron 54:197–203. https://doi.org/10.1016/j.orgel.2017.12.050
48. Zhong Z, Lian H, Wu J et al (2018) Efficient blue phosphorescent organic light-emitting diodes enabled by ag-nanoparticles-embedded hole transporting layer. Org Electron 56:31–36. https://doi.org/10.1016/j.orgel.2018.01.021
49. Cai Y, Shi C, Zhang H et al (2018) Sulfur-bridged tetraphenylethylene AIEgens for deep-blue organic light-emitting diodes. J Mater Chem C 6:6534–6542. https://doi.org/10.1039/C8TC01509K
50. Yan Z, Wang Y, Ding J et al (2017) Methoxyl modification in furo[3,2-c]pyridine-based iridium complexes towards highly efficient green- and orange-emitting electrophosphorescent devices. J Mater Chem C 5:12221–12227. https://doi.org/10.1039/C7TC04269H
51. Kumar S, Surati KR, Lawrence R et al (2017) Design and synthesis of heteroleptic iridium(III) phosphors for efficient organic light-emitting devices. Inorg Chem 56:15304–15313. https://doi.org/10.1021/acs.inorgchem.7b02872
52. Esteruelas MA, Gómez-Bautista D, López AM et al (2017) η1-Arene complexes as intermediates in the preparation of molecular phosphorescent iridium(III) complexes. Chem Eur J 23:15729–15737. https://doi.org/10.1002/chem.201703252
53. Shi C, Li Q, Zou L et al (2018) A single-anion-based red-emitting cationic diiridium(III) complex bearing a pyrimidine-based bridging ligand for oxygen sensing. Eur J Inorg Chem 2018:1131–1136. https://doi.org/10.1002/ejic.201800004
54. Hu W-K, Li S-H, Ma X-F et al (2018) Blue-to-green electrophosphorescence from iridium(III) complexes with cyclometalated pyrimidine ligands. Dyes Pigments 150:284–292. https://doi.org/10.1016/j.dyepig.2017.12.020
55. Li J, Tian Z, Xu Z et al (2018) Highly potent half-sandwich iridium and ruthenium complexes as lysosome-targeted imaging and anticancer agents. Dalton Trans 47:15772–15782. https://doi.org/10.1039/C8DT02963F
56. Miao Y, Tao P, Gao L et al (2018) Highly efficient chlorine functionalized blue iridium(III) phosphors for blue and white phosphorescent organic light-emitting diodes with the external quantum efficiency exceeding 20%. J Mater Chem C 6:6656–6665. https://doi.org/10.1039/C8TC01098F
57. Zanoni KPS, Ito A, Grüner M et al (2018) Photophysical dynamics of the efficient emission and photosensitization of [Ir(pqi)2(NN)]+ complexes. Dalton Trans 47:1179–1188. https://doi.org/10.1039/C7DT03930A
58. Molaee H, Nabavizadeh SM, Jamshidi M et al (2017) Phosphorescent heterobimetallic complexes involving platinum(IV) and rhenium(VII) centers connected by an unsupported μ-oxido bridge. Dalton Trans 46:16077–16088. https://doi.org/10.1039/C7DT03126B
59. Congrave DG, Batsanov AS, Du M et al (2018) Intramolecular π–π interactions with a chiral auxiliary ligand control Diastereoselectivity in a Cyclometalated Ir(III) complex. Inorg Chem 57:12836–12849. https://doi.org/10.1021/acs.inorgchem.8b02034

60. Zou J, Wu H, Lam C-S et al (2011) Simultaneous optimization of charge-carrier balance and luminous efficacy in highly efficient white polymer light-emitting devices. Adv Mater 23:2976–2980. https://doi.org/10.1002/adma.201101130
61. Baranoff E, Fantacci S, De Angelis F et al (2011) Cyclometalated iridium(III) complexes based on phenyl-imidazole ligand. Inorg Chem 50:451–462. https://doi.org/10.1021/ic901834v
62. Park H-R, Ha Y (2012) Introduction of the benzoquinoline ancillary ligand to the iridium complexes for organic light-emitting diodes. J Nanosci Nanotechnol 12:1365–1370
63. Karatsu T, Nakamura T, Yagai S et al (2003) Photochemical mer → fac one-way isomerization of phosphorescent material. Studies by time-resolved spectroscopy for Tris[2-(4′,6′-difluorophenyl)pyridine]iridium(III) in solution. Chem Lett 32:886–887. https://doi.org/10.1246/cl.2003.886
64. Laskar IR, Hsu S-F, Chen T-M (2005) Syntheses, photoluminescence and electroluminescence of some new blue-emitting phosphorescent iridium(III)-based materials. Polyhedron 24:189–200. https://doi.org/10.1016/j.poly.2004.10.016
65. McDonald AR, Lutz M, von Chrzanowski LS et al (2008) Probing the mer- to fac-isomerization of tris-cyclometallated homo- and heteroleptic (C,N)3 iridium(III) complexes. Inorg Chem 47:6681–6691. https://doi.org/10.1021/ic800169n
66. Tsuchiya K, Ito E, Yagai S et al (2009) Chirality in the photochemical mer→fac geometrical isomerization of Tris(1-phenylpyrazolato,N,C2′)iridium(III). Eur J Inorg Chem 2009:2104–2109. https://doi.org/10.1002/ejic.200801254
67. Becke AD (1993) Density-functional thermochemistry. III. The role of exact exchange. J Chem Phys 98:5648–5652. https://doi.org/10.1063/1.464913
68. Stephens PJ, Devlin FJ, Chabalowski CF, Frisch MJ (1994) Ab initio calculation of vibrational absorption and circular dichroism spectra using density functional force fields. J Phys Chem 98:11623–11627. https://doi.org/10.1021/j100096a001
69. Kim K, Jordan KD (1994) Comparison of density functional and MP2 calculations on the water monomer and dimer. J Phys Chem 98:10089–10094. https://doi.org/10.1021/j100091a024
70. Clark T, Chandrasekhar J, Spitznagel GW, Schleyer PVR (1983) Efficient diffuse function-augmented basis sets for anion calculations. III. The 3-21+G basis set for first-row elements, Li–F. J Comput Chem 4:294–301. https://doi.org/10.1002/jcc.540040303
71. Zhao Y, Truhlar DG (2008) The M06 suite of density functionals for main group thermochemistry, thermochemical kinetics, noncovalent interactions, excited states, and transition elements: two new functionals and systematic testing of four M06-class functionals and 12 other functionals. Theor Chem Accounts 120:215–241. https://doi.org/10.1007/s00214-007-0310-x
72. Chai J-D, Head-Gordon M (2008) Systematic optimization of long-range corrected hybrid density functionals. J Chem Phys 128:084106. https://doi.org/10.1063/1.2834918
73. Francl MM, Pietro WJ, Hehre WJ et al (1982) Self-consistent molecular orbital methods. XXIII. A polarization-type basis set for second-row elements. J Chem Phys 77:3654–3665. https://doi.org/10.1063/1.444267
74. Hay PJ, Wadt WR (1985) Ab initio effective core potentials for molecular calculations. Potentials for the transition metal atoms Sc to Hg. J Chem Phys 82:270–283. https://doi.org/10.1063/1.448799
75. Cancès E, Mennucci B, Tomasi J (1997) A new integral equation formalism for the polarizable continuum model: theoretical background and applications to isotropic and anisotropic dielectrics. J Chem Phys 107:3032–3041. https://doi.org/10.1063/1.474659
76. Mennucci B, Tomasi J (1997) Continuum solvation models: a new approach to the problem of solute's charge distribution and cavity boundaries. J Chem Phys 106:5151–5158. https://doi.org/10.1063/1.473558
77. Cossi M, Barone V, Mennucci B, Tomasi J (1998) Ab initio study of ionic solutions by a polarizable continuum dielectric model. Chem Phys Lett 286:253–260. https://doi.org/10.1016/S0009-2614(98)00106-7
78. Witkowska E, Wiosna-Salyga G, Glowacki I et al (2018) Effect of fluorine substitution of the β-ketoiminate ancillary ligand on photophysical properties and electroluminescence ability of new iridium(III) complexes. J Mater Chem C 6:8688–8708. https://doi.org/10.1039/C8TC02890G
79. Orwat B, Witkowska E, Kownacki I et al (2017) Microwave-assisted one-pot synthesis of new ionic iridium complexes of [Ir(bzq)2(N^N)]+a− type and their selected electroluminescent properties. Dalton Trans 46:9210–9226. https://doi.org/10.1039/C7DT01372H
80. Frisch MJ, Trucks GW, Schlegel HB et al (2016) Gaussian16 revision B.01. Gaussian Inc, Wallingford
81. Lamansky S, Djurovich P, Murphy D et al (2001) Synthesis and characterization of phosphorescent cyclometalated iridium complexes. Inorg Chem 40:1704–1711. https://doi.org/10.1021/ic0008969
82. Konno H, Ito T, Sugita Y (2013) Method for producing complex of trisortho-metalated iridium, light-emitting material using said complex, and light-emitting element. Patent: US9200023
83. Daniels RE, Culham S, Hunter M et al (2016) When two are better than one: bright phosphorescence from non-stereogenic dinuclear iridium(III) complexes. Dalton Trans 45:6949–6962. https://doi.org/10.1039/C6DT00881J
84. González I, Dreyse P, Cortés-Arriagada D et al (2015) A comparative study of Ir(III) complexes with pyrazino[2,3-f][1,10]phenanthroline and pyrazino[2,3-f][4,7]phenanthroline ligands in light-emitting electrochemical cells (LECs). Dalton Trans 44:14771–14781. https://doi.org/10.1039/C5DT01385B
85. Henwood AF, Pal AK, Cordes DB et al (2017) Blue-emitting cationic iridium(III) complexes featuring pyridylpyrimidine ligands and their use in sky-blue electroluminescent devices. J Mater Chem C 5:9638–9650. https://doi.org/10.1039/C7TC03110F
86. Frey J, Curchod BFE, Scopelliti R et al (2014) Structure–property relationships based on Hammett constants in cyclometalated iridium(III) complexes: their application to the design of a fluorine-free FIrPic-like emitter. Dalton Trans 43:5667–5679. https://doi.org/10.1039/C3DT52739E
87. Liu X, Zhang S, Jin Y-M et al (2015) Syntheses, crystal structure and photophysical property of iridium complexes with 1,3,4-oxadiazole and 1,3,4-thiadiazole derivatives as ancillary ligands. J Organomet Chem 785:11–18. https://doi.org/10.1016/j.jorganchem.2015.02.025
88. Jing Y-M, Zheng Y-X (2017) Photoluminescence and electroluminescence of deep red iridium(III) complexes with 2,3-diphenylquinoxaline derivatives and 1,3,4-oxadiazole derivatives ligands. RSC Adv 7:37021–37031. https://doi.org/10.1039/C7RA05530G
89. Chen L, Doeven EH, Wilson DJD et al (2017) Co-reactant electrogenerated chemiluminescence of iridium(III) complexes containing an acetylacetonate ligand. ChemElectroChem 4:1797–1808. https://doi.org/10.1002/celc.201700222
90. González I, Cortés-Arriagada D, Dreyse P et al (2015) A family of IrIII complexes with high nonlinear optical response and their potential use in light-emitting devices. Eur J Inorg Chem 2015:4946–4955. https://doi.org/10.1002/ejic.201500505